THESIS FOR THE DEGREE OF LICENTIATE OF ENGINEERING

# Advanced Dual Circularly Polarized Antenna for Automotive Sensing Radar

Zhaorui Zang


CHALMERS
UNIVERSITY OF TECHNOLOGY

Department of Electrical Engineering
Chalmers University of Technology
Gothenburg, Sweden, 2022

**Advanced Dual Circularly Polarized Antenna for Automotive Radar Systems**

Zhaorui Zang



Department of Electrical Engineering
Chalmers University of Technology
SE-412 96 Gothenburg, Sweden
Phone: +46 (0)31 772 1000
www.chalmers.se

Printed by Chalmers Reproservice
Gothenburg, Sweden, October 2022

*To my family*

# Abstract

Advanced driver assistance systems (ADAS) promise reliable support for collision avoidance and cruise control. The demand for precise target classification and road surface sensing requires a sensor revolution. In this regard, the automotive radar system is highly expected to collect as much information as possible. Especially, polarimetric radar systems have shown an advantage for sensing and imaging. Automotive polarimetric radar requires an advanced antenna system with high polarimetric capabilities, relatively small size, high efficiency, and low-cost for mass production.

This thesis presents several 77 GHz advanced antenna models for various ranges of automotive polarimetric radar systems. Gap waveguide technology has been used to design two single-layer dual circular polarized antenna arrays, which are suitable for automotive radar applications. The first antenna is a dual circularly polarized low profile 8×1 array with wide impedance bandwidth and axial ratio bandwidth (11 %), high port isolation (18.6 dB), and moderate gain (14.8 dBi). The second design presented is an 18×8 series fed planar array which is designed based on the leaky-wave principle and has about 3.9 % bandwidth with 27.3 dBi gain. The achieved port isolation is better than 17.5 dB.

The proposed antenna arrays can be easily integrated with the commercial radar chip by using simple microstrip to gap waveguide transition. Therefore a fully functional polarimetric radar front-end could be designed in the future.



**Keywords:** Antenna, gap waveguide, automotive, radar, low-profile, dual circular polarization, polarimetric radar.

# List of Publications

This thesis is based on the following publications:

[A] **Zhaorui Zang**, Ashraf Uz Zaman, Jian Yang, Carlo Bencivenni, Konstantinos Konstantinidis, "Single Layer Dual Circularly Polarized Antenna Elements for Automotive Radar at 77 GHz". *2021 15th European Conference on Antennas and Propagation (EuCAP)*, 2021, pp. 1-4.
 DOI: 10.23919/EuCAP51087.2021.9411028 .

[B] **Zhaorui Zang**, Ashraf Uz Zaman, Jian Yang, "Single Layer Dual Circularly Polarized Antenna Array Based on Ridge Gap Waveguide for 77 GHz Automotive Radar". *Published by IEEE Transactions on Antennas and Propagation* .

[C] **Zhaorui Zang**, Ashraf Uz Zaman, Jian Yang, "Design of Dual Circularly Polarized Inclined Slot Pair Based on Stepped-Height Ridge Gap Waveguide with Series Excitation". *2022 15th European Conference on Antennas and Propagation (EuCAP)*, 2021, pp. 1-5.
 DOI: 10.23919/EuCAP53622.2022.9768998 .

[D] **Zhaorui Zang**, Ashraf Uz Zaman, Jian Yang, "Single Layer Dual Circularly Polarized Series-fed Gap Waveguide Based Slot Array for 77 GHz Automotive Radar". *Submitted to IEEE Transactions on Antennas and Propagation* .

# Acknowledgments

I would like to express my sincere appreciation to my main supervisor, Associate Prof. Ashraf Uz Zaman, for his constant guidance and unwavering support for this project. I am extremely grateful to my examiner, Prof. Jian Yang, for his constructive suggestions during the project. I would also like to thank my manager Prof. Marianna V. Ivashina, for all the enjoyable discussions we had. I am also grateful to Dr. Oleg Iupikov, and Dr. Pavlo Krasov for their assistance in simulation and measurement for this project.

Many thanks to my co-supervisor, Dr. Carlo Bencivenni, who is from Gapwaves AB, for his ingenious suggestions and supports on measurement. Thank Dr. Konstantinos Konstantinidis, from Veoneer Germany GmbH, for the support and feedback during this project. Special thanks to everyone involved in the FORWARD project, Associate Prof. Vessen Vassilev from the Department of Microtechnology and Nanoscience, Dr. Esperanza Alfonso and Marcus Hasselblad from Gapwaves, Robert Moestam from CEVT, and Olof Eriksson from Veoneer, for their generous engagement and efforts in this project.

I very much appreciate the colleagues at the Department of Electrical Engineering for the friendly and comfortable work environment. I also wish to thank my friends at Antenna Systems for their help and support during these years.

It is a special story for me to study in Chalmers during the epidemic. Thanks to all my friends who supported and helped me to feel not alone in Göteborg. Many thanks to Ivan, who supported me all the time.

To the friends and family in my home country, Many thanks, and I miss you a lot. Hope to see you soon.

Zhaorui
Göteborg, October 2022

# Acronyms

| | |
|---|---|
| ADAS: | Advanced driver assistance systems |
| LiDAR: | Light detection and ranging |
| ACC: | Adaptive cruise control |
| LRR: | Long-range radar |
| MRR: | Medium-range radar |
| SRR: | Short-range radar |
| DBF: | Digital beam forming |
| PolSAR: | Polarimetric synthetic aperture radar |
| FMCW: | Frequency-modulated continuous-wave |
| PCB: | Print circuit board |
| LP: | Linearly polarized |
| CP: | Circularly polarized |
| MIMO: | Multi input Multi output |
| mmWave: | millimeter wave |
| PEC: | Perfect electric conductor |
| PMC: | Perfect magnetic conductor |
| GGW: | Groove gap waveguide |
| RGW: | Ridge gap waveguide |
| IMGW: | Inverted microstrip gap waveguide |
| RHCP: | Right hand circular polarization |
| LHCP: | Left hand circular polarization |

| | |
|---|---|
| AR: | Axial ratio |
| ARBW: | Axial ratio bandwidth |
| IMBW: | Impedance bandwidth |
| SIW: | substrate integrated waveguide |
| BFNs: | Beamforming networks |

# Contents

# Part I

# Overview

# CHAPTER 1

# Introduction

## 1.1 Motivation

Modern vehicles with assistance for safe driving become a major interest in recent years. In the beginning, researchers have focused on the functionality of avoiding a crash. Adaptive cruise control (ACC), and automatic emergency brake (AEB) systems are developed widely with this consideration. Currently, a concept of advanced driver assistance systems (ADAS) has been proposed to provide more functions for pedestrians/ cyclists detection, long-range sensing and road environment monitoring [1]–[4]. To this end, sensor systems, which are considered the eyes of modern vehicles, are expected to get as much, detailed information as possible for the ADAS [5]–[7]. Conventionally, the sensor system consists of ultrasonic, radars, LiDARs, and passive visual (cameras). The comparison of different sensors is shown in Fig. 1.1.

Compared with other sensor systems, radars shows advantages in proximity detection, working in different weather, and detecting speed. What's more, the digital beam forming (DBF), multiple-input multiple-output (MIMO) technology, and advanced data processing allow radar systems to achieve more possibilities for road surface detection and target classification. In that regard,

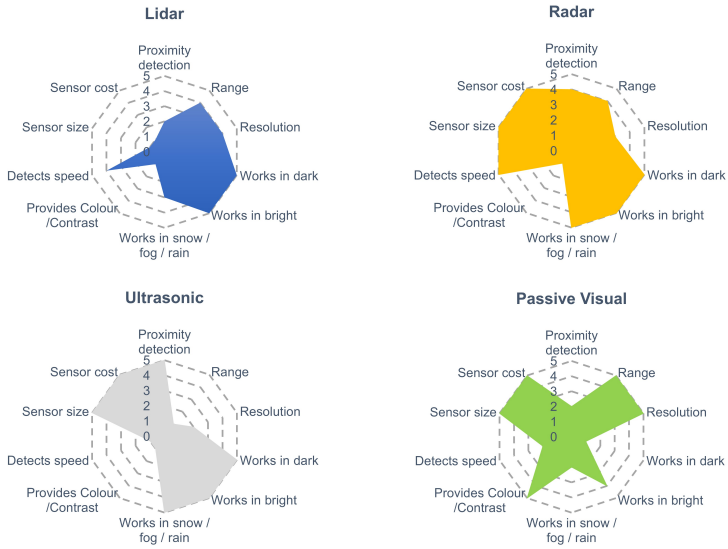


**Figure 1.1:** Characteristics comparison of different sensors [6].

many commercial automotive radars are designed. Regarding the operating range, they are classified into three types: short-range radar (SRR), mid-range radar (MRR), and long-range radar (LRR), as shown in Fig. 1.2.

Conventionally, the SRR is mounted on the rear and side of a vehicle and mainly works for Side-Crash and Parking. The MRR is mounted on the front grille, bumper, or air vents of the car for AEB systems and detecting vehicle cut-ins. The LRR has a similar position as MRR while mainly working for maintaining headway with the vehicle head and ACC systems.

Nowadays, most types of automotive sensing radar systems are aimed to detect and collect as much information as possible from the target objects. However, systems with linear polarization cannot detect low cross-section objects precisely. Moreover, it highly depends on the scattering orientation of objects. Thus, a radar system having different polarization on transmitter and receiver is necessary for automotive sensing applications. In this regard, fully-polarimetric radar could be considered.

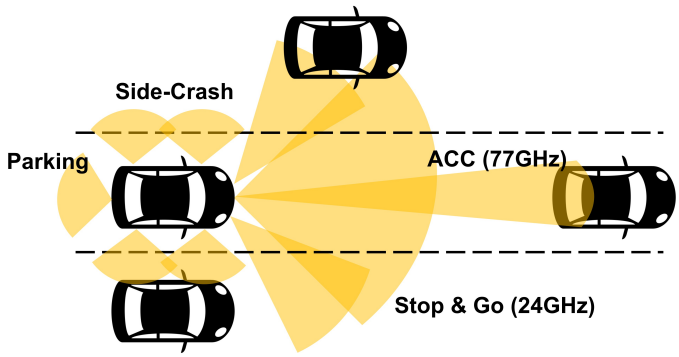


| | Freq. | BW | Modulation | Angle | Range | Resolution | Application |
|---|---|---|---|---|---|---|---|
| Short-Range | 24 GHz | 7 GHz | Pulsed | 70° | 10 m | < 10 cm | Side-Crash & Parking |
| Mid-Range | 24 GHz | 250 MHz | FMCW | 30°~60° | 40 m | ~ 1 m | Stop & Go |
| Long-Range | 77 GHz | 1 GHz | FMCW | 16° | 150 m | ~ 1 m | ACC |

**Figure 1.2:** Classification of different automotive sensing radar types [6].

## 1.2 Polarimetric radar for automotive applications

As mentioned above, polarimetric radar utilizes different polarizations at transmitter and receiver. It has a long and rich history for remote sensing and imaging applications as permitting more inference information from natural surfaces and targets than radar systems with a single polarization. Weather conditions such as atmosphere ice particles, hydrometeor classification, and quantification can be estimated by a full polarimetric radar, which characterizes differential propagation phase, linear depolarization ratio, and/or differential reflectivity [8], [9]. On another hand, systems like polarimetric synthetic aperture radar (PolSAR) can image the earth's surface by measuring a scattering matrix $S$, which preserves the physical scattering properties of the polarization-changing targets (ocean, traffic area or so)[10].

Polarimetric radar normally uses different polarizations on the transmitter and receiver. To mathematically describe the coherent polarization state of an EM wave [10], it is necessary to introduce the Jones vectors, which are denoted by

$$\vec{E}_J = \begin{pmatrix} E_{0x}e^{j\phi_x} \\ E_{0y}e^{j\phi_y} \end{pmatrix}. \tag{1.1}$$

All polarization states can be described with a simple notation by Jones vectors. For example, $(1/\sqrt[2]{2}, -j/\sqrt[2]{2})^T$ could describe a right-hand circular polarization. To describe the connections to the incident and scattered Jones vectors, S-matrix is introduced in [11], [12]. At a location $A$, the incident and scattered Jones vector is

$$\vec{E}_{Js} = \frac{e^{-j\vec{k}\vec{r}}}{\sqrt{4\pi}|\vec{r}|} \begin{pmatrix} S_{11} & S_{12} \\ S_{21} & S_{22} \end{pmatrix} \vec{E}_{Ji} = \frac{e^{-j\vec{k}\vec{r}}}{\sqrt{4\pi}r} S\vec{E}_{Ji}, \tag{1.2}$$

where $r$ is the distance between the source of the Jones vector and the target, $S$ is the scattering S-matrix, and $E_{Js}$ is the scattered Jones vector at location $A$. Since the S-matrix can be expressed with orthogonal polarizations, the S-matrix can be written as:

$$S = e^{j\phi_{hh}} \begin{pmatrix} |S_{hh}| & |S_{hv}|e^{j(\phi_{hv}-\phi_{hh})} \\ |S_{vh}|e^{j(\phi_{vh}-\phi_{hh})} & |S_{vv}|e^{j(\phi_{vv}-\phi_{hh})} \end{pmatrix}, \tag{1.3}$$

where horizontal and vertical polarization has been used and the S-matrix is expressed with magnitude and phase. The matrix shows that both the phases and magnitudes of information entries are evaluated, which means polarimetric radar has more capabilities to collect information than single polarized radar.

Nevertheless, there are lots of advantages and literature about polarimetric radar, it is noted that they are seldom implied to automotive applications in the early past 20 years. Fig. 1.3 shows that the citation quantity of polarimetric radar is arising every year since 2000, and is almost 16000 by now. However, as shown in Fig. 1.4, the citations of polarimetric radar for automotive applications are only around 50 now. The comparison between Fig. 1.3 and Fig. 1.4 demonstrates the area of automotive polarimetric radar is almost blank, which shows huge potential for research and commercial design.

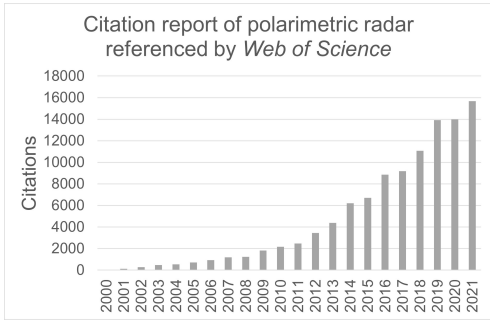


**Figure 1.3:** Citation report of polarimetric radar referenced by Web of Science.

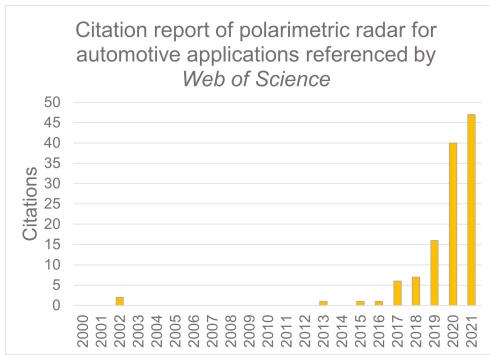


**Figure 1.4:** Citation report of polarimetric radar for automotive applications referenced by Web of Science.

## 1.3 Antenna challenges for automotive radar

To explain the main technological challenges of antenna design for automotive applications in detail, it is necessary to show some antenna prototypes from some commercial radar boards, as shown in Fig. 1.5, Fig. 1.6 and Fig. 1.7.

Fig. 1.5 shows the photograph of frequency-modulated continuous-wave (FMCW) radar boards from TI and NXP. Both of them had 3 transmitters and 4 receivers. Each transmitter and receiver consisted of one series-fed patch antenna array. The series-fed patch antenna array is the most popular choice for automotive applications for its flexibility in lower fabrication cost. They are also easy to integrate with millimeter wave and microwave circuits.

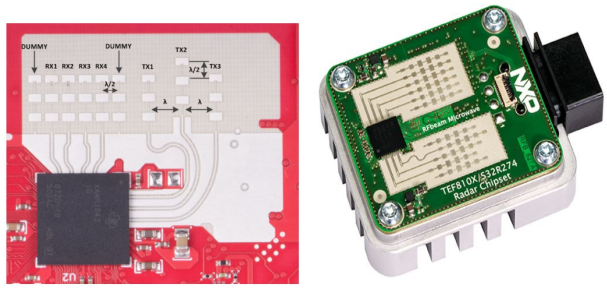


**Figure 1.5:** Linear patch antenna arrays of TI and NXP [13], [14].

However, series-fed patch antenna array suffers the high dielectric loss and working frequency band shift problems at millimeter wave (mmWave).

Fig. 1.6 shows the photograph of reflectarray antennas of ARS300 and Conti ADC. Reflectarray antenna is mainly developed for multibeam with a cheaper solution. Fig. 1.7 shows the photograph of LRR FMCW radar from Bosch. The lens was fed by four single patch antennas and achieved four narrow beams. Generally, a lens can simplify the patch antenna size and enhance the capabilities for beam shaping. Compared to a phased array antenna, the lens antenna requires fewer switches and active components. However, both the reflectarray and the lens antenna face similar problems as the series-fed patch antenna, and dielectric loss, since most of them use dielectric material. On another hand, reflect array and lens tend to be bulky in volume, which is not always desired.

Regarding these, the challenges could be concluded to three aspects:

- Material Loss.
- Compact antenna arrangements.
- Production cost and assembly challenges.

Firstly, material loss. It contains the dielectric loss and the conductor loss of the PCB. Generally speaking, dielectric losses are associated with the dissipation factor ($D_f$) of the PCB substrate. On the other hand, conductor loss is contributed by the skin depth and surface roughness of the conductor. These losses are unneglectable at a higher frequency, not only for the

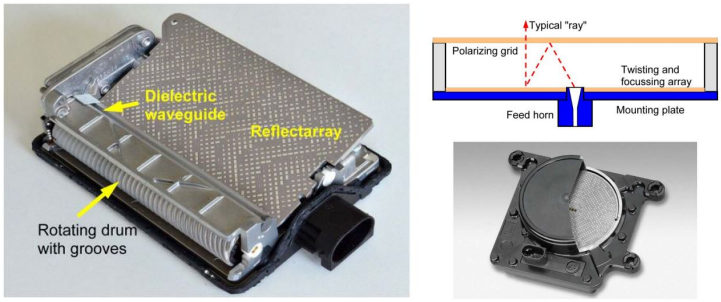


**Figure 1.6:** Reflectarray of ARS300 and Conti ADC [15].

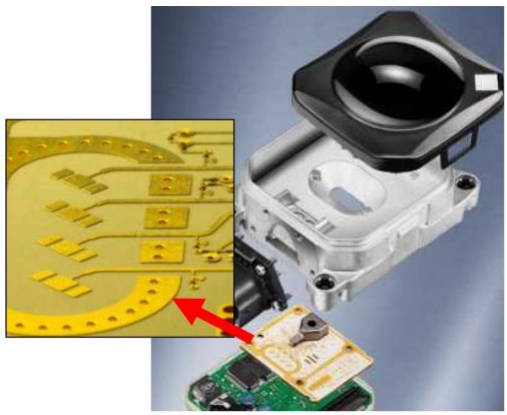

**Figure 1.7:** Lens antenna of Bosch [16].

substrate-build antennas but for onboard-routing lines. Nevertheless, electroplating techniques could reduce the conductor loss, the dielectric loss becomes extremely stupendous for antennas with more complex geometry [17].

Secondly, compact antenna arrangements. As the sensor has to be integrated into the car, the overall dimensions of the radar boards are relatively small and should have low profiles. Thus, a low-profile high-gain compact antenna arrangement is necessary.

Finally, production cost and assembly challenges. Automotive sensing radar must suit low-cost mass production. In this regard, some low-loss dielectric

substrates are unsuitable for their high cost. Meanwhile, technology like multiple layers substrates normally requires complex machining processes, which makes it unattractive for automotive applications.

## 1.4 Gap waveguide technology

Gap waveguide technology (GW) is widely investigated in recent 10 years as a solution to avoid dielectric loss at mmWave [18]–[24]. The working theory of GW is based on the soft surface and hard surface. The basic idea is, the wave propagation will be forbidden at the soft surface area while enhanced at the hard surface area. In this way, the wave is only allowed to propagate along a desired path within the GW. The soft surface could be achieved by placing periodic metallic pins or mushrooms within a parallel plate waveguide. The hard surface could be achieved by some guiding lines. It is noted that the air gap should be lower than a quarter of $\lambda$, which is the space between the top plate of the parallel plate waveguide and the perfect magnetic conductor (PMC) surface.

According to the types of guiding lines, GW could be classified into four types: ridge gap waveguide (RGW), groove gap waveguide (GGW), inverted microstrip gap waveguide (IMGW), and microstrip-ridge gap waveguide. Their geometry is shown in Fig. 1.8. It is noted that there is a quasi-TEM mode propagating along the RGW, IMGW, and microstrip-ridge gap waveguide, While $TE_{10}$ mode along GGW as shown in 1.9. On the other hand, both the RGW and GGW are all metallic built while substrates are needed for IMGW and microstrip-ridge gap waveguide.

On another hand, integrating RF electronics with the GW has been a challenge in the mmWave frequency range. Several low-loss integration concepts have been proposed over the last few years. In [25] a complete E-band Front-end with an integrated transmitter and receiver MMIC has been demonstrated based on multi-layer geometry. In [26], [27], several transitions from microstrip to GW have been proposed and all these transitions show low-loss performance in the mmWave range. Also, the manufacturing of GW antennas and components is less expensive than conventional waveguides. No electric contact requirement between the metal layers makes it suitable for low-cost manufacturing such as die-sink EDM, 3D printing, polymer injection molding, and micromachining techniques [28]–[31].

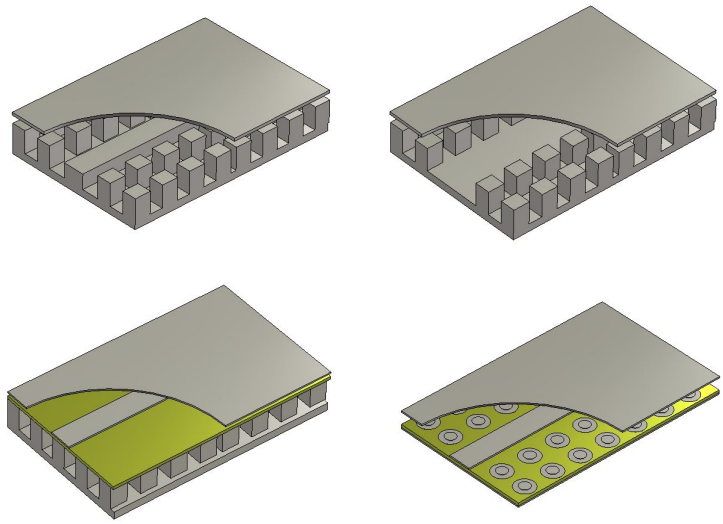

**Figure 1.8:** Different gap waveguide geometries [18].

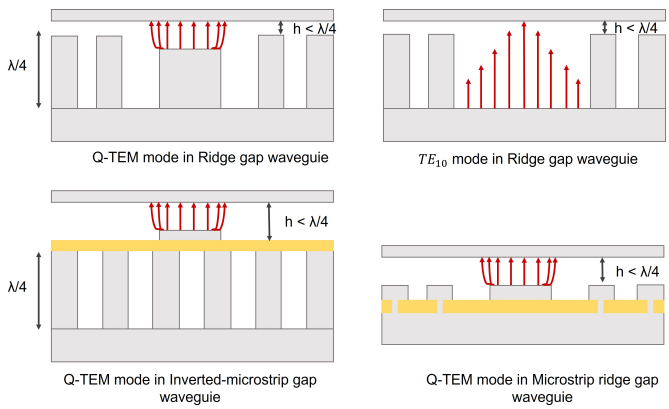


**Figure 1.9:** Desired modes of propagation in different gap waveguide geometries [18].

## 1.5 Goals and objectives

This research aims to develop novel gap waveguide based dual CP antenna for automotive radar applications at mmWave. Several research objectives have been set to achieve this goal:

- Develop advanced single layer gap waveguide antenna with dual circular polarization for SRR/MRR applications at 77 GHz automotive band.
- Develop high gain single layer dual CP antenna at 77 GHz band for LRR applications.

Throughout this project, we aim to develop simple and single layer low-cost gap waveguide based dual CP antenna array with relative impedance bandwidth and axial ratio bandwidth of 3 %-4 % at 77 GHz band.

## 1.6 Thesis outline

**Chapter** 2 overviews the approahes to realize a dual CP antenna at mmWave. A low-profile RGW based dual CP antenna is proposed in **Chapter** 3. A advanced series-fed dual CP antenna is proposed in **Chapter** 4 for LRR application. The summary of included papers is shown in **Chapter** 6.

# CHAPTER 2

# Dual Circularly Polarized Antenna at Millimeter Wave

This chapter gives an overview of different approaches to developing a dual CP antenna for automotive polarimetric radar at mmWave. Some examples are summarized, and their advantages and disadvantages are discussed.

## 2.1 Overview of dual CP antenna

The polarization of an antenna is dependent on the orientation of its radiated electric fields [32]. The electric field could be written as

$$\vec{E}(\theta,\varphi) = \vec{\theta}E_\theta(\theta,\varphi)e^{j\Phi_1} + \vec{\varphi}E_\varphi(\theta,\varphi)e^{j\Phi_2} \tag{2.1}$$

where $E_\theta(\theta,\varphi)$ and $E_\varphi(\theta,\varphi)$ denote the magnitudes of electric field of the far field, $\Phi_1$ and $\Phi_2$ are the phase shift of each component.

Circularly polarized wave has orthogonal field components with almost equal magnitudes, orthogonal spatially, and quadrature phase. That is

$$\begin{aligned} E_\theta(\theta,\varphi) &= E_\varphi(\theta,\varphi) \\ \Phi_1 - \Phi_2 &= \pm\frac{\pi}{2} \end{aligned} \tag{2.2}$$

Different from a linear polarized wave, whose tip of the electric field vector oscillates along the same line, the CP wave tip of the resultant electric field vector generates a circular locus while evolving in time, as shown in Fig. 2.1. When the field rotation is clockwise, it is known as right-hand circularly polarized (RHCP). Otherwise, it is left-hand circularly polarized (LHCP).

Axial ratio ($AR$) is used to quantify the CP performance and is given in decibels by:

$$AR(dB) = 20log_{10}|\frac{E_{max}}{E_{min}}|, \tag{2.3}$$

where $E_{max}$ and $E_{min}$ are the maximum and minimum semi-axes of the polarization ellipse. A frequency range when $AR \leq$3 dB is defined as Axial Ratio Bandwidth ($ARBW$):

$$ARBW = \frac{[f_2 - f_1]}{f_0}, \tag{2.4}$$

where, $f_1$ and $f_2$ are the boundary frequencies for $AR \leq$3 dB, and $f_0$ is the center frequency.

There could be mainly two types of dual CP antenna. One is realizing dual CP at different frequency bands simultaneously, the other one is achieving dual CP separately at the same frequency bands. In this research, we focus on the second type.

There are various approaches for an antenna element to realize a dual CP performance. Design approaches such as two asymmetry-fed radiators and differentially fed dipoles have been investigated a lot, as shown in Fig. 2.2. However, most of them are operating at a low frequency. When the frequency band moves to mmWave, the geometry of them are relatively tiny, and the SMA coaxial RF connector is lossy, which makes them unsuitable to be used [33]–[36].

## 2.2 Challenges of dual CP antenna at mmWave

At mmWave, approaches such as metasurface, a sequential-phase feeding network, a hybrid coupler, and multiple-layer geometry are always utilized to realize the dual CP performance. The comparison of some examples is shown in Table 2.1.

A dual CP radiation array was proposed in [37] based on substrate integrated waveguide (SIW) technology. The integrated power splitting network contained several phase shifters and 3 dB couplers. This antenna had a single layer geometry with 18.2 % impedance bandwidth and 17% axial ratio bandwidth. However, it is unsuitable for automotive radar applications due to the complex feeding network.

In [38], SIW based cavity-back slot antennas array was developed with sequential rotation feeding technique. Wideband performance (nearly 32.3 % impedance bandwidth) was achieved by loading metasurface layers above the slot. But it had orbital angular momentum beams, which shows low capabilities to be used in automotive radar systems.

A GW-based switchable dual CP antenna array was realized in [39]. Thanks to its all-metal structure, the dielectric loss was avoided. However, the slot array was fed by a standing wave, which meant that manual actions were needed to switch the polarization. It would be difficult to implement such solution for automotive radars.

In [40], a dual circularly-polarized (CP) multibeam antenna was proposed based on pillbox reflector beamforming networks (BFNs) and series-fed patch antenna array for 24 GHz automotive radar. About $\pm 36^\circ$ beam scanning range was achieved with a gain higher than 17.7 dBi. However, it only had about 4.17 % impedance bandwidth and the double-layer substrates (Rogers 4003C) are relatively expensive. Based on the series-fed working form, a single-layer dual CP antenna was proposed in [41]. Although it provided lower dielectric loss than the parallel-fed antenna, the array aperture was too large to be applied to automotive radar systems.

Some multiple-layer dual CP antenna array was designed based on hybrid coupler in [42] and [43]. Both of them had high efficiency but multiple-layer geometry was relatively bulky and hard to integrate with radar chips which have multiple channels.

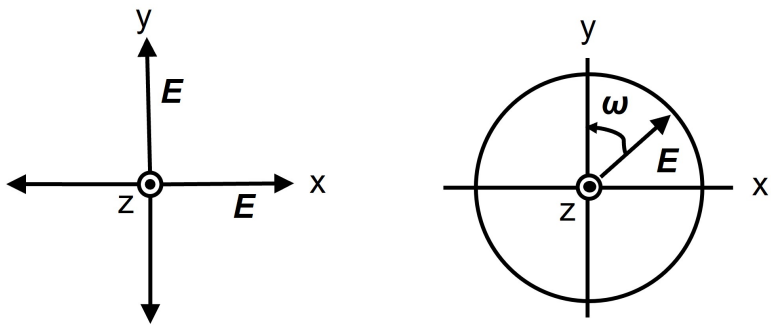


**Figure 2.1:** Electric field vector tracing [32].

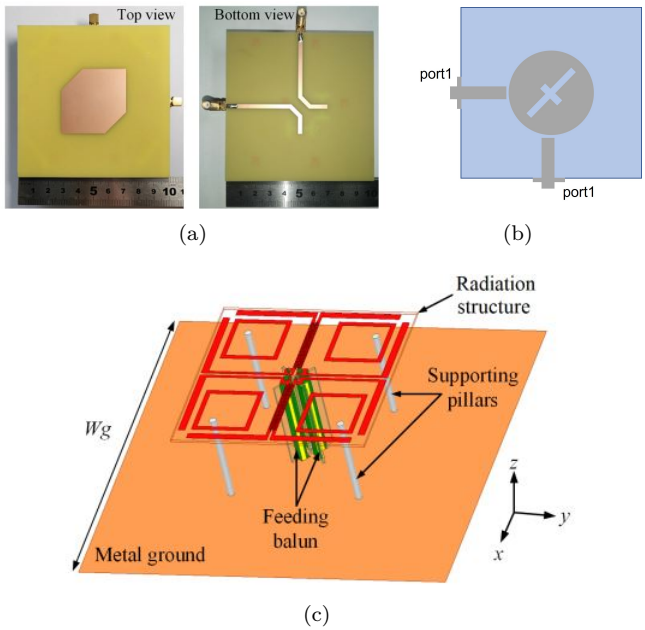


**Figure 2.2:** Various approaches to realized dual CP (a) asymmetry fed radiators[33], (b) asymmetry fed radiators[34], (c) differential fed dipoles[35].

## 2.3 Novelty of this thesis

Instead of implying complex couplers in the feeding network and multiple-layer geometry, this work for the first time presents two low-profile low-cost dual CP antenna solutions for various types of automotive sensing radar with simple geometry. Two antenna elements and arrays are proposed, fabricated, and measured. The results are fully analyzed in the attached papers.

**Table 2.1:** Previous work and design challenges

| Ref. | Implement solutions | Freq (GHz) | Challenges |
|---|---|---|---|
| [37] 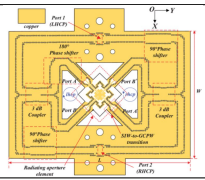 | SIW, phase shifter | 60 | Feeding network unsuitable for automotive radar |
| [38] 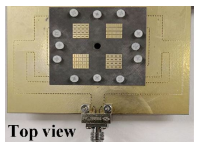  | Metasurface and sequentially rotated feeding | 30 | Dielectric loss and orbital angular momentum beams |
| [39] 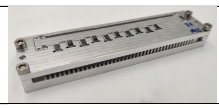 | Gap Waveguide | 30 | Manually switch the dual circular polarizations |
| [40] 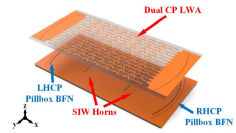  | SIW, series-feeding | 24 | Dielectric loss and narrow bandwidth |
| [41] 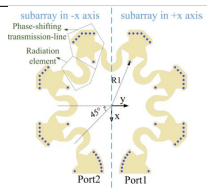  | Sequential rotation, series-feeding | 30 | Dielectric loss and large geometry size |
| [42] 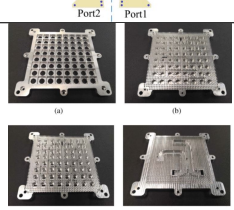 | Gap Waveguide, hybrid coupler | 30 | Multiple layers and large geometry size |
| [43] 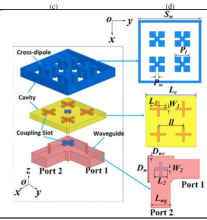  | 3D printing, hybrid coupler | 26 | Multiple layers and large geometry size |

# CHAPTER 3

# Advanced Dual Circularly Polarized (CP) Antenna for SRR/MRR Applications

A single-layer dual circularly polarized antenna array based on ridge gap waveguide is proposed, manufactured, and measured in this chapter for SRR/LRR applications.

## 3.1 Design specifications for SRR and MRR applications

While normally the SRR and MRR have different angular resolutions and coverage ranges, there are no formulated specific definitions and distinctions between them. For antenna systems, it is possible to design an antenna both for SRR and MRR applications. Regarding the widely accepted requirements of commercial SRR/ MRR FMCW radar, some specifications are assumed in this work for the dual CP antenna system, as shown in Table 3.1.

**Table 3.1:** Proposed specifications for SRR/MRR antenna.

| Required properties | Target value |
|---|---|
| Polarizations | Dual CP |
| Working frequency band | 76-81 GHz |
| Axial ratio | $\leq$3 dB |
| X-pol. level | $\leq$-20 dB |
| Layers number | 1 |

## 3.2 Low profile dual CP antenna array

As mentioned before, an asymmetric-fed radiator could achieve a dual CP performance. Especially, there exists a structure named U-shaped slot [44], which has two asymmetric-fed microstrip lines and one U-shaped asymmetric aperture, as shown in Fig. 3.1. Both the feeding lines and the aperture contribute to the circular polarization performance. As a result, wide axial ratio bandwidth (ARBW) could be achieved. However, this geometry face problem of port isolation and back radiation.

Based on the U-shaped aperture, an RGW-based U-shaped slot element is proposed in this work, as shown in Fig. 3.2. The U-shaped slot is located on the top plate of RGW and is fed by two ridges that are excited separately. By carefully tuning the geometrical parameters $S$ and $L$, high port isolation and good CP performance are achieved. The RGW not only avoids the dielectric loss but also avoids the back radiation, which is problematic for automotive sensing radar systems.

The RGW-based U-shaped slot element shows the potential to be integrated with a radar chip for its lightweight and single-layer geometry. The slot element is used to design a 8-element linear array with two feeding networks, which contains two 1-to-8 power dividers and two WG-to-RGW transitions, as shown in Fig. 3.3. The prototype is built with brass with dimensions of 42×50×6.2 mm and is fed by two WR-12 waveguide ports. Both S-parameters and far field measurements are done with a measurement setup shown in Fig. 3.4. The far field patterns are shown in Fig. 3.5. It shows that the proposed antenna achieves a stable pattern and lower relative cross-polarization level (X-pol. level). The design detail and results analysis is presented in **Paper A** and **Paper B**.

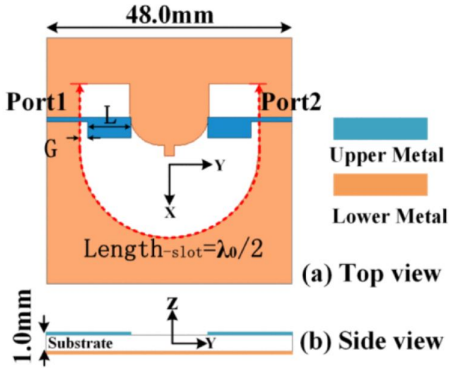


**Figure 3.1:** U-shaped slot geometry[44]

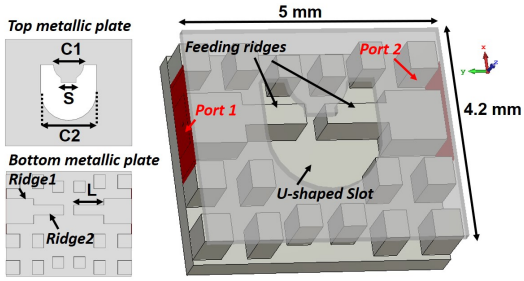


**Figure 3.2:** RGW based U-shaped slot geometry.

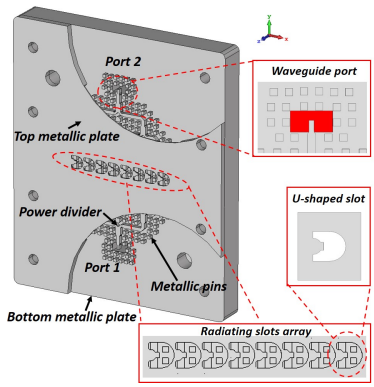


**Figure 3.3:** Overall model of the proposed dual CP antenna array.

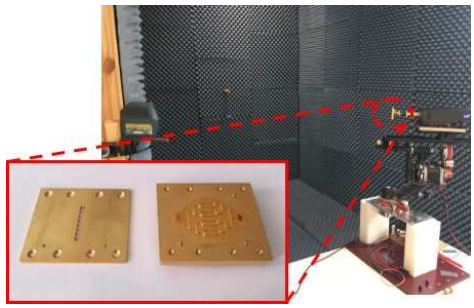

**Figure 3.4:** Far field measurements set-up.

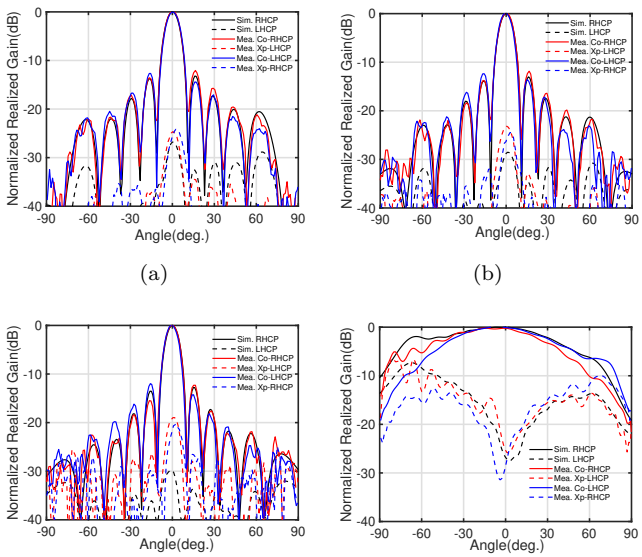


**Figure 3.5:** Normalized simulated and measured patterns on $xz/yz$ plane at different frequencies. (a) 76 GHz. (b) 78.5 GHz. (c) 81 GHz. (a) 76 GHz on $yz$ plane.

# CHAPTER 4

# Advanced Dual CP Antenna for LRR Applications

This chapter presents a novel approach for designing a series-fed dual CP antenna on stepped RGW. An 18-element linear array design example is proposed and realized. Based on it, a planar array is simulated, manufactured, and measured.

## 4.1 Design specifications for LRR applications

Compared to SRR and MRR applications, for antenna systems, the LRR usually requires larger gain and higher beam scanning capabilities to cover a relatively long range in fort of the vehicle [45]. In this regard, more antenna elements and smaller array separation are necessary for each transmitter and receiver. The specifications of the dual CP antenna system for the LRR application are shown in Table 4.1.

**Table 4.1:** Proposed specifications for LRR antenna system

| Required properties | Target value |
|---|---|
| Polarizations | Dual CP |
| Impedance bandwidth (IBW) | 76-79 GHz |
| Axial Ratio bandwidth (ARBW) | 76-79 GHz |
| Port isolation | $\geq$ 15 dB |
| Array lengths | $\leq$ 60 mm |
| Layers number | $\leq 2$ |
| Realized gain | $\geq$ 24 dBi |
| Gain variation over frequency band | $\leq$ 2 dB |
| Side lobe level (SLL) | $\leq -12$ dB |
| Grating lobe level | $\leq -20$ dB |
| X-pol. level | $\leq -20$ dB |

## 4.2 Series-fed waveguide slot antenna array

Waveguide slot antenna array was developed and improved for many years. Most people follow Elliott's framework for the design process [46]–[49]. Generally, according to the feeding mechanism, waveguide slot antenna is categorized into two basic types: standing wave slot arrays and traveling wave slot arrays (series-fed slot arrays).

For standing wave slot arrays with slot spacing d=$\lambda_g/2$, the design equations are:

$$\frac{Z_n^a}{Z_0} = \frac{K_1 f(\theta_n, l_n) V_n^s}{I_n}, \tag{4.1}$$

where $Z_n^a$ is the active impedance of the $n$ slot and $Z_0$ is the characteristics impedance of waveguides with different modes. $I_n$ is the mode current of the $n$ slot, and $V_n^s$ is the maximum voltage at the center of the $n$ slot. Normally, for the $\lambda_g/2$ spacing slot, the $I_n$ value is common to all elements. Thus, following Equation 4.1, the array could be easily defined with a specific pattern.

However, for the $\lambda_g$ spacing series-fed slot array, the magnitude of mode

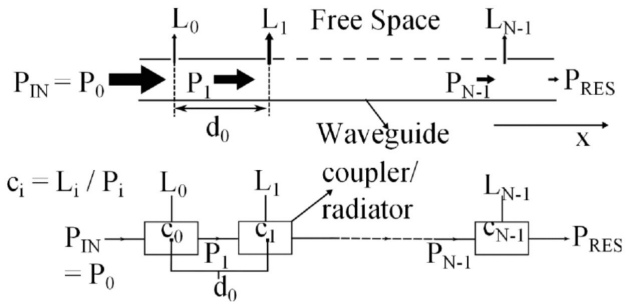


**Figure 4.1:** Coupling factors model [50].

current is no longer equal for all elements, since some power is radiated out by former slots. In this regard, the coupling factors model is utilized in this work to design the series-fed array, as shown in Fig. 4.1. $P_{in}$ is the input power, $P_n$ is the residual power, $L_n$ is the radiated power and $C_n$ is defined as the coupling factor of $n$ slot. It notes that each slot in the array should keep an under-coupling state, which means the radiation efficiency of each element is relatively small so most of the power is transmitted to the remaining slots in the array. Based on the coupling factor model, a 24-element dual CP slot array was realized for satellite applications, as shown in Fig.4.2.

Compared to standing wave slot arrays, series-fed slot arrays have wider impedance and more potential to realize dual polarizations by feeding from two ports separately.

## 4.3 Stepped RGW

As discussed in Section 1.4, there is a quasi-TEM mode wave propagating along the ridge within the RGW. [24] shows that the dispersion of the quasi-TEM mode wave is almost similar as the light line, which means the guided wavelength ($\lambda_g$) is nearly equal to $\lambda_0$.

On the other hand, for series-fed slot array design, to achieve broadside radiation, the slot should be located with a space of $\lambda_g$. However, for a linear array design, a larger side lobe and grating lobe may appear when the element space is chosen nearly $\lambda_0$. As a result, some new designs are needed to decrease

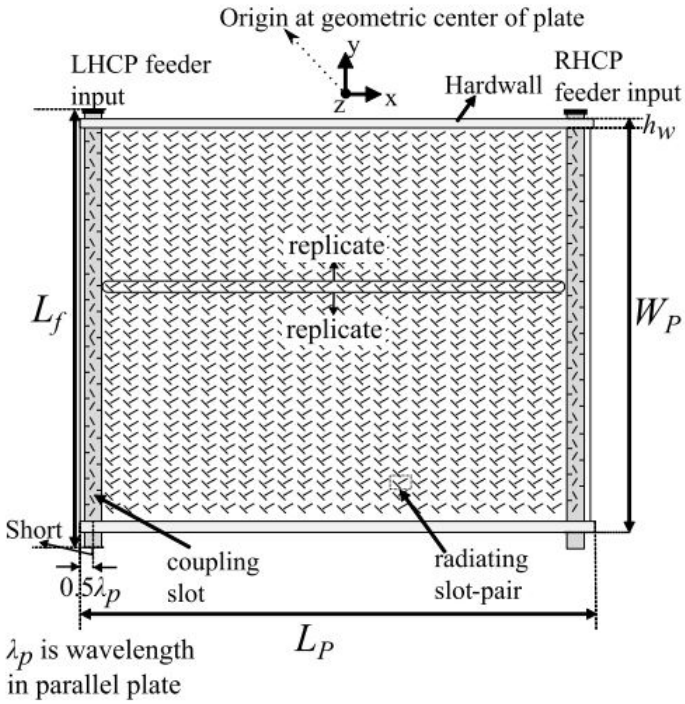


**Figure 4.2:** Geometry of a honeycomb-based dual CP antenna array [50].

the $\lambda_g$ within RGW.

Approaches such as honeycomb, dielectric-filled waveguide, and substrate integrated waveguide (SIW) have been well developed to decrease $\lambda_g$ within a waveguide. In [51], a periodic honeycomb with permittivity 1.06 was proposed to fill in a parallel plate waveguide, as shown in Fig. 4.3. Fig. 4.4 showed that the loss is relatively small at 9.65 GHz. SIW technology is chosen to decrease the $\lambda_g$ in [52], [53], as shown in Fig 4.5. However, at the mmWave frequency band, the honeycomb is hard to fabricate and the dielectric loss of SIW is relatively high. In this regard, stepped RGW is a good solution. Different from conventional RGW, there are periodic steps cut on the ridge of stepped RGW, as shown in Fig. 4.6. These steps increase the propagation path of the transmitting wave and decrease the $\lambda_g$.

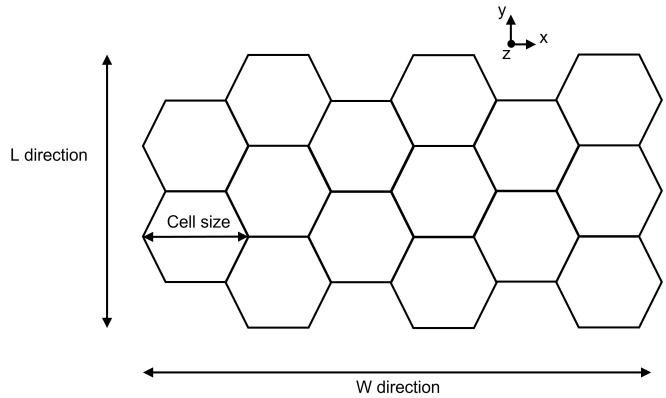


**Figure 4.3:** Geometry of honeycomb [51].

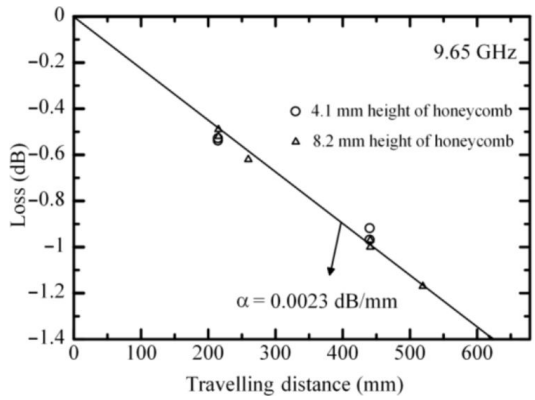


**Figure 4.4:** Measured honeycomb loss at 9.65 GHz [51].

## 4.4 Dual CP antenna array on stepped RGW

To realize the specifications of the LRR antenna, it is necessary to propose a waveguide slot element with good dual CP performance. In this regard, the inclined slot pair is considered to be a potential candidate for its dual CP property [54], [55].

The inclined slot pair contains two interacting radiating slots with a tilting angle $\theta_1$ and $\theta_2$ and are located on the broad wall of a waveguide, as shown

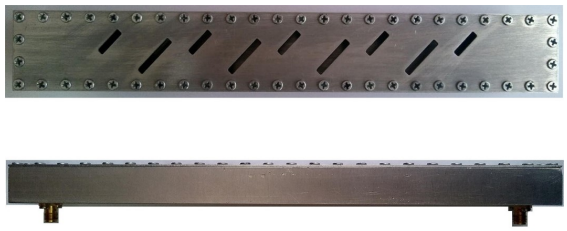

(a)

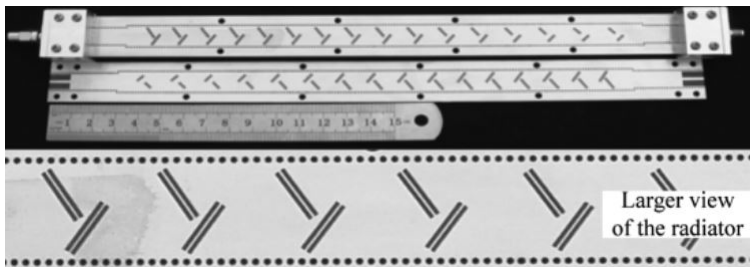


(b)

**Figure 4.5:** Series-fed waveguide slot array based on SIW (a) LP array, (b) CP array [52], [53].

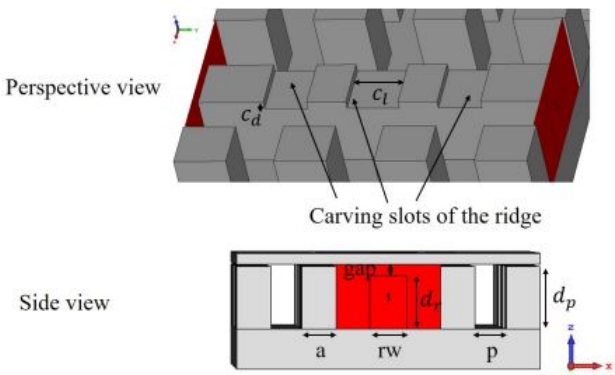


**Figure 4.6:** Geometry of the proposed stepped RGW.

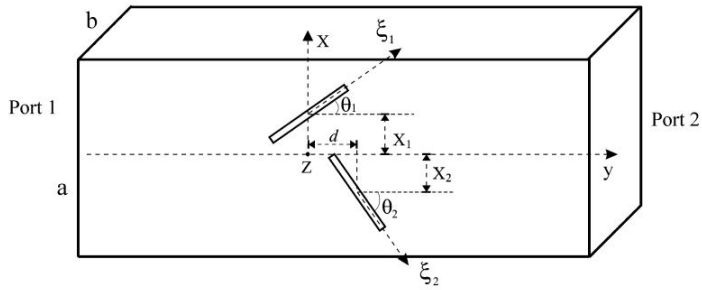


**Figure 4.7:** Inclined slot pair geometry[54].

in Fig. 4.7. Normally, the $\theta$ is equal to 45 °. The space between slots ($d$) is about a quarter of $\lambda_g$, which generates about 90 ° phase differences between the two slots. Basically, by tuning the location offsets ($X_1$ and $X_2$) from the center line of the waveguide, the slots could be excited by the current with equal magnitude. In this way, circular polarization is realized and the CP performance could be optimized by tuning all of the parameters above. When fed from port 1, an LHCP is realized. Contrarily, an RHCP is realized when port 2 is excited.

Based on the inclined slot pair, [54] derived an effective method of moments (MoM) code for slot array design. However, since the near field of the slots interacts with each other, the independent analysis is not enough for this slot pair. What's more, the MoM procedure is hard to be applied to stepped RGW as there is no commonly accepted analytical field solution available for the stepped RGW. These two challenges make it harder to design an inclined slot element on stepped RGW with the method proposed in [54].

Regarding this difficulty, we for the first time propose a design flow for the stepped RGW-based inclined slot element by utilizing commercial software (CST Studio Suite). Based on the simulation data and curves, a series-fed dual CP inclined slot array is developed and optimized by a full wave simulation. The novel design process is shown in Fig. 4.8. To achieve higher antenna gain, an 8-column planar array is proposed and the planar array is excited by two 1-to-8 power dividers and two WG-to-RGW transitions. The overall model geometry is shown in Fig. 4.9. Fig. 4.10 describes the far field measurement setup. For more details please refer to **Paper C** and **Paper D**.

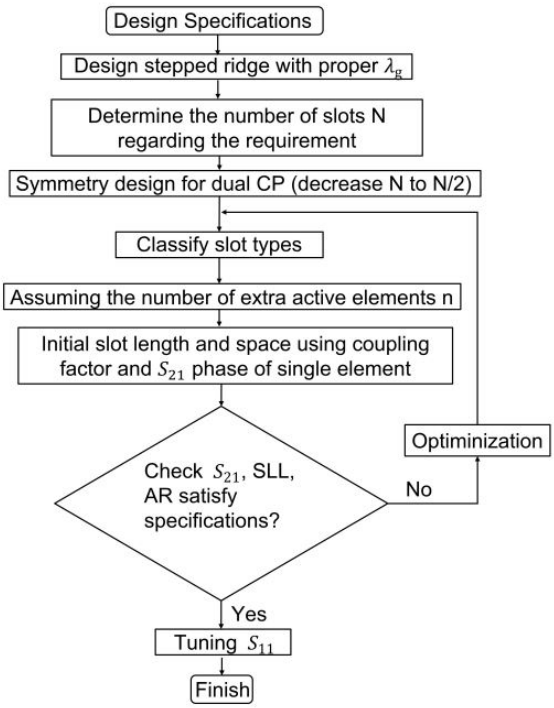


**Figure 4.8:** Design process of the series-fed dual CP antenna array.

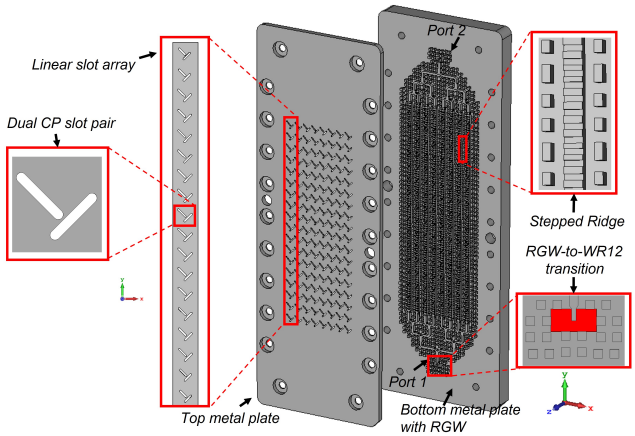


**Figure 4.9:** Overall geometry of proposed antenna.

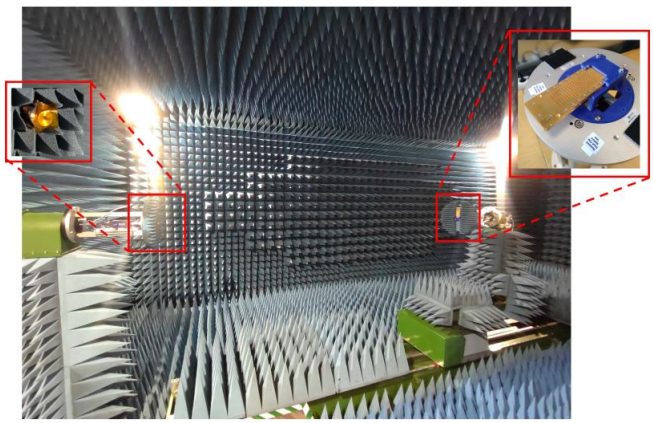

**Figure 4.10:** Far field measurements set-up.

# CHAPTER 5

# Summary of included papers

This chapter provides a summary of the included papers.

## 5.1 Paper A

**Zhaorui Zang**, Ashraf Uz Zaman, Jian Yang, Carlo Bencivenni, Konstantinos Konstantinidis
Single Layer Dual Circularly Polarized Antenna Elements for Automotive Radar at 77 GHz
*2021 15th European Conference on Antennas and Propagation (EuCAP)*, 2021, pp. 1-4.
 DOI: 10.23919/EuCAP51087.2021.9411028.

In this paper, two different configurations of dual circularly polarized antenna elements in single layer gap waveguide (GW) are presented for 77GHz automotive radar systems. Both of the antenna configurations utilize slot element to radiate and generate circular polarizations. The right-hand circular polarization (RHCP) and the left-hand circular polarization (LHCP) are generated at the same working frequency with different input ports. The sim-

ulated results show that both two antenna elements could cover the proposed impedance bandwidth (75-80 GHz) with an axial ratio lower than 2 dB.

## 5.2 Paper B

**Zhaorui Zang**, Ashraf Uz Zaman, Jian Yang
Single Layer Dual Circularly Polarized Antenna Array Based on Ridge Gap Waveguide for 77 GHz Automotive Radar
*Published by IEEE Transactions on Antennas and Propagation.*

A single layer 77 GHz dual circularly polarized (CP) antenna array is proposed based on ridge gap waveguides (RGWs) technology. The antenna consists of eight U-shaped slots, fed by two feeding networks for generation of dual CP. The proposed antenna array has been fabricated and measured. The experimental results show good agreement with the simulations. The axial ratio is below 2 dB, and the return loss and port isolation are better than 13 and 18.6 dB over 76–81 GHz, respectively. The measured gain for the integrated array is 14.8 dBi at the center frequency of 78.5 GHz. With integration of feeding networks and the radiating elements in a single layer, this antenna has potential to be used in automotive radars.

## 5.3 Paper C

**Zhaorui Zang**, Ashraf Uz Zaman, Jian Yang
Design of Dual Circularly Polarized Inclined Slot Pair Based on Stepped-Height Ridge Gap Waveguide with Series Excitation
*2022 15th European Conference on Antennas and Propagation (EuCAP)*, 2021, pp. 1-5.
 DOI: 10.23919/EuCAP53622.2022.9768998.

This paper presents a new stepped-height ridge structure to reduce the guided wavelength of a conventional ridge gap waveguide. Compared to other technology, the stepped-height ridge gap waveguide avoids dielectric loss and reduces the manufacturing cost. The simulation results prove that the guided wavelength could be decreased sufficiently by adjusting the step numbers and step depth. Based on this structure, a dual circularly polarized inclined slot

pair is investigated and simulated. The slot pair is located on the top plate of the ridge gap waveguide and is fed by a traveling wave. The simulation results show that the inclined slot pair could generate a good dual circular polarization with the axial ratio below 3 dB over 76-81 GHz. The discrete models of the inclined slot pair are also shown in this paper.

## 5.4 Paper D

**Zhaorui Zang**, Ashraf Uz Zaman, Jian Yang
Single Layer Dual Circularly Polarized Series-fed Gap Waveguide Based Slot Array for 77 GHz Automotive Radar
*Submitted to IEEE Transactions on Antennas and Propagation.*

A series-fed slot array antenna fed by stepped ridge gap waveguide is proposed at the 77 GHz band. The antenna generates dual circularly polarized waves, which shows potential to be used in next-generation polarimetric radar for automotive applications. The antenna contains 8 columns of linear arrays and two feeding ports for exciting the columns of the slots. The design process and measured results are described in this paper. The measured results show that the realized gain of the proposed antenna is above 27.3 dBi over the proposed 76-79 GHz with dual CP patterns. The measured $S_{11}$ and $S_{22}$ for the proposed antenna are below -10 dB and the measured axial ratio is about 2 dB over the proposed frequency band.

# CHAPTER 6

# Concluding Remarks and Future Works

## 6.1 Conclusion

To develop polarimetric radar for automotive sensing systems, an advanced antenna is needed to provide dual circular polarization. In this thesis, we have proposed two low-profile dual CP antenna models, which can be integrated directly with radar chips at a relatively low cost for mass production.

An RGW based single layer dual CP antenna array was demonstrated in **Chapter** 3 for SRR/ MRR applications at 77 GHz. High efficiency (75.9 %-84.7 %) and good dual CP performance (AR$\leq$ 2 dB) are achieved at a frequency band of 76-81 GHz.

A stepped RGW-based series-fed single layer antenna array is presented in **Chapter** 4 for dual CP LRR applications. We propose a design flow for a stepped RGW based series-fed slot array. Based on this, an 8-column planar array is proposed and measured, which shows potential to be integrated into radar boards.

## 6.2 Future work

It has been demonstrated that the proposed antenna models have excellent electrical performance and the potential to be integrated into commercial radar chips. In the future, based on these antenna models, we prepare to build a polarimetric FMCW radar front-end with a circular polarized antenna array based on gap waveguide technology.

# References


[1] R. P, "Toward a fully integrated automotive radar system-on-chip in 22 nm fd-soi cmos," *International Journal of Microwave and Wireless Technologies*, vol. 14, no. 6, pp. 523–531, 2021.

[2] J. Hasch, E. Topak, R. Schnabel, T. Zwick, R. Weigel, and C. Waldschmidt, "Millimeter-wave technology for automotive radar sensors in the 77 ghz frequency band," *IEEE Transactions on Antennas and Propagation*, vol. 60, no. 3, pp. 845–860, 2012.

[3] K. A. Mishra M, "Adas technology: A review on challenges, legal risk mitigation and solutions," *Autonomous Driving and Advanced Driver-Assistance Systems (ADAS)*, pp. 401–408, 2021.

[4] B. A. Jumaa, A. M. Abdulhassan, and A. M. Abdulhassan, "Advanced driver assistance system (adas): A review of systems and technologies," *International Journal of Advanced Research in Computer Engineering & Technology (IJARCET)*, vol. 8, no. 6, 2019.

[5] E. Marti, M. A. De Miguel, F. Garcia, and J. Perez, "A review of sensor technologies for perception in automated driving," *IEEE Intelligent Transportation Systems Magazine*, vol. 11, no. 4, pp. 94–108, 2019.

[6] B. Béchadergue, "Visible light range-finding and communication using the automotive led lighting," 2017.

[7] C. Waldschmidt, J. Hasch, and W. Menzel, "Automotive radar—from first efforts to future systems," *IEEE Journal of Microwaves*, vol. 1, no. 1, pp. 135–148, 2021.

[8] J. Vivekanandan, V. N. Bringi, M. Hagen, and P. Meischner, "Polarimetric radar studies of atmospheric ice particles," *IEEE transactions on geoscience and remote sensing*, vol. 32, no. 1, pp. 1–10, 1994.

[9] J. M. Straka, D. S. Zrnić, and A. V. Ryzhkov, "Bulk hydrometeor classification and quantification using polarimetric radar data: Synthesis of relations," *Journal of Applied Meteorology*, vol. 39, no. 8, pp. 1341–1372, 2000.

[10] S. Otgonbaatar and M. Datcu, "Natural embedding of the stokes parameters of polarimetric synthetic aperture radar images in a gate-based quantum computer," *IEEE Transactions on Geoscience and Remote Sensing*, vol. 60, pp. 1–8, 2021.

[11] T. Visentin, "Polarimetric radar for automotive applications," *KIT Scientific Publishing*, vol. 90, 2019.

[12] S. Trummer, G. F. Hamberger, U. Siart, and T. F. Eibert, "A polarimetrie 76–79 ghz radar-frontend for target classification in automotive use," *2016 46th European Microwave Conference (EuMC)*, vol. 1, pp. 1493–1496, 2016.

[13] T. Instruments, "Awr1843aop single-chip 77- and 79-ghz fmcw mmwave sensor antennas-onpackage (aop)," *TI datasheet*, vol. 1, pp. 1–21, 2019.

[14] N. Semiconductors, "Tef810x fully-integrated 77 ghz radar transceiver," vol. 1, 2019.

[15] D. P. W. Menzel and M. Al-Tikriti, "Mm-wave folded reflector antennas with high gain, low loss, and low profile," *IEEE Antennas Propagation Mag.*, vol. 67, pp. 24–29, 2002.

[16] W. Menzel and A. Moebius, "Antenna concepts for millimeter-wave automotive radar sensors," *Proceedings of the IEEE*, vol. 100, no. 7, pp. 2372–2379, 2012.

[17] T. G. J. Mayer M. Martina and T. Zwick, "Pcb laminates for automotive radar antenna modules under different environmental conditions," *IEEE Transactions on Antennas and Propagation*, vol. 67, no. 9, pp. 6051–6058, 2019.

[18] A. Uz and P.-S. Kildal, "Wide-band slot antenna arrays with single-layer corporate-feed network in ridge gap waveguide technology," *IEEE Transactions on Antennas and Propagation*, vol. 62, no. 6, pp. 2992–3001, 2014.

[19] P.-S. Kildal, A. U. Zaman, E. Rajo-Iglesias, E. Alfonso, and A. Valero-Nogueira, "Design and experimental verification of ridge gap waveguide in bed of nails for parallel-plate mode suppression," *IET Microwaves, Antennas & Propagation*, vol. 5, no. 3, pp. 262–270, 2011.

[20] J. Liu, A. Vosoogh, A. U. Zaman, and J. Yang, "A slot array antenna with single-layered corporate-feed based on ridge gap waveguide in the 60 ghz band," *IEEE Transactions on Antennas and Propagation*, vol. 67, no. 3, pp. 1650–1658, 2018.

[21] E. Rajo-Iglesias, M. Ferrando-Rocher, and A. U. Zaman, "Gap waveguide technology for millimeter-wave antenna systems," *IEEE Transactions on Antennas and Propagation*, vol. 56, no. 7, pp. 14–20, 2018.

[22] A. Vosoogh, A. Haddadi, A. U. Zaman, J. Yang, H. Zirath, and A. A. Kishk, "W-band low-profile monopulse slot array antenna based on gap waveguide corporate-feed network," *IEEE Transactions on Antennas and Propagation*, vol. 66, no. 12, pp. 6997–7009, 2018.

[23] A. Vosoogh, M. S. Sorkherizi, A. U. Zaman, J. Yang, and A. A. Kishk, "An integrated ka-band diplexer-antenna array module based on gap waveguide technology with simple mechanical assembly and no electrical contact requirements," *IEEE Transactions on Microwave Theory and Techniques*, vol. 66, no. 2, pp. 962–972, 2017.

[24] H. Raza, J. Yang, P.-S. Kildal, and E. Alfonso, "Resemblance between gap waveguides and hollow waveguides," *IET Microwaves, Antennas & Propagation*, vol. 7, no. 15, pp. 1221–1227, 2013.

[25] A. Vosoogh, M. Sharifi Sorkherizi, V. Vassilev, *et al.*, "Compact integrated full-duplex gap waveguide-based radio front end for multi-gbit/s point-to-point backhaul links at e-band," *IEEE Transactions on Microwave Theory and Techniques*, vol. 67, no. 9, pp. 3783–3797, 2019.

[26] U. Nandi, A. U. Zaman, A. Vosoogh, and J. Yang, "Novel millimeter wave transition from microstrip line to groove gap waveguide for mmic packaging and antenna integration," *IEEE Microwave and Wireless Components Letters*, vol. 27, no. 8, pp. 691–693, 2017.

[27] Q. Ren, A. U. Zaman, J. Yang, V. Vassilev, and C. Bencivenni, "Novel integration techniques for gap waveguides and mmics suitable for multi-layer waveguide applications," *IEEE Transactions on Microwave Theory and Techniques*, vol. 70, no. 9, pp. 4120–4128, 2022.

[28] A. Vosoogh, P.-S. Kildal, and V. Vassilev, "A multi-layer gap waveguide array antenna suitable for manufactured by die-sink edm," *IEEE 10th European Conference on Antennas and Propagation (EuCAP)*, vol. 1, pp. 1–4, 2016.

[29] A. Tamayo-Domínguez, J.-M. Fernández-González, and M. Sierra-Pérez, "Groove gap waveguide in 3-d printed technology for low loss, weight, and cost distribution networks," *IEEE Transactions on Microwave Theory and Techniques*, vol. 65, no. 11, pp. 4138–4147, 2017.

[30] S. Farjana, M. Ghaderi, A. U. Zaman, *et al.*, "Realizing a 140 ghz gap waveguide–based array antenna by low-cost injection molding and micromachining," *Journal of Infrared, Millimeter, and Terahertz Waves*, vol. 42, no. 8, pp. 893–914, 2021.

[31] S. Farjana, M. Ghaderi, A. U. Zaman, S. Rahiminejad, P. Lundgren, and P. Enoksson, "Low-loss gap waveguide transmission line and transitions at 220–320 ghz using dry film micromachining," *IEEE Transactions on Components, Packaging and Manufacturing Technology*, vol. 11, no. 11, pp. 2012–2021, 2021.

[32] B. Y. Toh, R. Cahill, and V. F. Fusco, "Understanding and measuring circular polarization," *IEEE Transactions on Education*, vol. 46, no. 3, pp. 313–318, 2003.

[33] S. Wang, D. Yang, W. Geyi, C. Zhao, and G. Ding, "Polarization-reconfigurable antenna using combination of circular polarized modes," *IEEE Access*, vol. 9, pp. 45 622–45 631, 2021.

[34] G.-L. Wu, W. Mu, G. Zhao, and Y.-C. Jiao, "A novel design of dual circularly polarized antenna fed by l-strip," *Progress In Electromagnetics Research*, vol. 79, pp. 39–46, 2008.

[35] H. D. Li, X. Y. Du, J. Y. Yin, J. Ren, and Y. z. Yin, "Differentially fed dual-circularly polarized antenna with slow wave delay lines," *IEEE Transactions on Antennas and Propagation*, vol. 68, no. 5, pp. 4066–4071, 2019.

[36] W. Chen, Z. Yu, J. Zhai, and J. Zhou, "Developing wideband dual-circularly polarized antenna with simple feeds using magnetoelectric dipoles," *IEEE Antennas and Wireless Propagation Letters*, vol. 19, no. 6, pp. 1037–1041, 2020.

[37] J. Zhu, S. Liao, Y. Yang, S. Li, and Q. Xue, "60 ghz dual-circularly polarized planar aperture antenna and array," *IEEE Transactions on Antennas and Propagation*, vol. 66, no. 2, pp. 1014–1019, 2017.

[38] J. Wu, Z. Huang, X. Ren, E. Wei, and X. Wu, "Wideband millimeter-wave dual-mode dual circularly polarized oam antenna using sequentially rotated feeding technique," *IEEE Antennas and Wireless Propagation Letters*, vol. 19, no. 8, pp. 1296–1300, 2020.

[39] M. Ferrando-Rocher, J. I. Herranz-Herruzo, A. Valero-Nogueira, and B. Bernardo-Clemente, "Switchable t-slot for dual-circularly-polarized slot-array antennas in ka-band," *IEEE Antennas and Wireless Propagation Letters*, vol. 20, no. 10, pp. 1953–1957, 2021.

[40] Y. Cao, S. Yan, J. Li, and J. Chen, "A pillbox based dual circularly-polarized millimeter-wave multi-beam antenna for future vehicular radar applications," *IEEE Transactions on Vehicular Technology*, 2022.

[41] Y.-H. Yang, B.-H. Sun, and J.-L. Guo, "A low-cost, single-layer, dual circularly polarized antenna for millimeter-wave applications," *IEEE Antennas and Wireless Propagation Letters*, vol. 18, no. 4, pp. 651–655, 2019.

[42] M. Ferrando-Rocher, J. I. Herranz-Herruzo, A. Valero-Nogueira, and B. Bernardo-Clemente, "Dual circularly polarized aperture array antenna in gap waveguide for high-efficiency ka-band satellite communications," *IEEE Open Journal of Antennas and Propagation*, vol. 1, pp. 283–289, 2020.

[43] B. Feng, Y. Tu, J. Chen, K. L. Chung, and S. Sun, "High-performance dual circularly-polarized antenna arrays using 3d printing for 5g millimetre-wave communications," *AEU-International Journal of Electronics and Communications*, vol. 130, p. 153 569, 2021.

[44] R. Xu, J.-Y. Li, J.-J. Yang, K. Wei, and Y.-X. Qi, "A design of u-shaped slot antenna with broadband dual circularly polarized radiation," *IEEE Transactions on Antennas and Propagation*, vol. 65, pp. 3217–3220, 2017.

[45] T. Kamimura, K. Kurashige, K. Yasooka, T. Suzuki, and Y. Tsubota, "Compact 76 ghz automotive long-range radar with high linearity chirp generator based on low phase noise open-loop vco," *16th European Radar Conference (EuRAD)*, vol. 1, pp. 125–128, 2019.

[46] R. Elliott, "An improved design procedure for small arrays of shunt slots," *IEEE Transactions on Antennas and Propagation*, vol. 3, no. 1, pp. 48–53, 1983.

[47] R. Elliott, "On the design of traveling-wave-fed longitudinal shunt slot arrays," *IEEE Transactions on Antennas and Propagation*, vol. 27, pp. 717–720, 1979.

[48] M. Orefice and R. Elliott, "Design of waveguide-fed series slot arrays," *IEE Proceedings H (Microwaves, Optics and Antennas)*, vol. 129, no. 4, pp. 165–169, 1982.

[49] G. Stern and R. Elliott, "Resonant length of longitudinal slots and validity of circuit representation: Theory and experiment," *IEEE Transactions on Antennas and Propagation*, vol. 33, no. 11, pp. 1264–1271, 1985.

[50] V. Ravindra, P. R. Akbar, M. Zhang, J. Hirokawa, H. Saito, and A. Oyama, "A dual-polarization $X$ -band traveling-wave antenna panel for small-satellite synthetic aperture radar," *IEEE Transactions on Antennas and Propagation*, vol. 65, no. 5, pp. 2144–2156, 2017.

[51] V. Ravindra, P. R. Akbar, M. Zhang, J. Hirokawa, H. Saito, and A. Oyama, "A dual-polarization $X$ -band traveling-wave antenna panel for small-satellite synthetic aperture radar," *IEEE Transactions on Antennas and Propagation*, vol. 65, no. 5, pp. 2144–2156, 2017.

[52] P. Chen, W. Hong, Z. Kuai, and J. Xu, "A substrate integrated waveguide circular polarized slot radiator and its linear array," *IEEE Antennas and Wireless Propagation Letters*, vol. 8, pp. 120–123, 2009.

[53] M. S. M. Meisam Dolati, "A wideband 45◦ inclined linear polarization travelling-wave slot array antenna with broadside radiation pattern," *International Journal of Electronics and Communications*, vol. 106, pp. 103–107, 2019.

[54] G. Montisci, M. Musa, and G. Mazzarella, "Waveguide slot antennas for circularly polarized radiated field," *IEEE Transactions on Antennas and Propagation*, vol. 52, no. 2, pp. 619–623, 2004.

[55] G. Montisci, "Design of circularly polarized waveguide slot linear arrays," *IEEE Transactions on Antennas and Propagation*, vol. 54, no. 10, pp. 3025–3029, 2006.